A computational study of the molecular and crystal structure and selected physical properties of octahydridosilasequioxane, $(Si_2O_3H_2)_4$. II. Vibrational Analysis.

C.J.H. Schutte[a] and J.A. Pretorius[b]

a Chemistry Department and Centre for Advanced Studies
b Chemistry Department and Supercomputer Centre
University of Pretoria
Hillcrest, Pretoria
South Africa

Abstract
A computational study of octahydridosilasequioxane, $Si_8O_{12}H_8$ as a free molecule and embedded in the unit cell *R*-3, *Z* = 3, showed that the point group of the free molecule is indeed O_h, but that its crystal symmetry is reduced to C_{3i}. Since the molecular and site-group symmetries influence the vibrational structure of a molecule, a full computational vibrational analysis of the isolated molecule and embedded in the crystal lattice is reported here. The analysis of the free molecular spectra given here agrees with that of its experimental IR-spectra and allows the assignment of all the vibrational modes, while the computed phonon dispersion of the crystal confirms the assignment of the internal vibrational modes of the molecule in the crystal. The computed and experimental infra-red and Raman spectra show no indication of serious vibrational intermolecular coupling due to the presence of multiple molecules in the unit cell. This may be the result of weak intermolecular vibrational coupling in the solid-state, which may feature in the low-frequency modes.

Keywords
octahydridosilasequioxane; silane; disiloxane; disilyl ether; infra-red; Raman

Abbreviations
MO - Molecular Orbital, AO - Atomic Orbital, DFT - Density Functional Theory, SMP - Shared Memory Processor, G03 - GAUSSIAN 03, PAW - Projector Augmented Wave method

1 Introduction

In Part I (Schutte and Pretorius 2011) it was pointed out that silicon compounds containing the [-Si-O-Si-] moiety play an important role in nature and science and technology. Recently, it was found that silicates even play a role in biochemistry; for instance, it was shown that silicon-like precipitates occur in the brain adjacent to neurons, which have been damaged by Parkinson's disease (Birchall and Chappell 1988; Bilinski *et al.* 1992); the nature of these aluminosilicates has not yet been determined, despite extensive research. On the technology side, despite massive research efforts, for instance, in zeolite catalysis, many open questions remain (Vora *et al* 1997; Wilson *et al.* 1999 and Seddon 2006). Pure SiO-based zeolites displaying continuous --Si--O--Si-- networks with similar or larger crystallographic asymmetric units (e.g. ZSM-5 or MFI) than octahydridosilasequioxane, exhibit structural areas with similar bond distances (1.62 Å) and bonding angles (147.9°). Although other enhanced areas displaying varying bond angles (101 - 176°) are also apparent within the same zeolite pore cavity, the highly selective nature of a few SiO-based zeolite catalysts also considering their shape selective capacities is indicative of a subtle underlying electron distribution. We attempt to initiate an exploration of such important electronic substructures in this paper, also referring to Part 1 of this series (Schutte and Pretorius 2011).

The following open questions with respect to octahydridosilasequioxane, still remain:

a) The close proximity of the sets of triangularly-packed hydrogen atoms in the unit cell raises the question: What are the partial charges on the hydrogen atoms? An effective partial charge estimate for the hydrogen atoms has been derived in Part I (Schutte and Pretorius 2011)?

b) Does the curious contradiction between the paucity of the IR-bands occurring in the spectrum of the solid-state and the expected 78 vibrational modes yield further information about the site symmetry of the molecule?

c) Can the fact that the vibrational spectra show almost no intermolecular coupling be related to the packing scheme?

On the scientific side structural aspects of silicate compounds were extensively investigated. But many questions remain, some of which were addressed by our computational study in Part I (Schutte and Pretorius 2011), where we showed that octahydridosilasequioxane can be considered to be representative of many different kinds of silicon-oxygen compounds, especially those that contain a hydrogen atom directly linked to a silicon atom. In Part I we give a full account of the important role that the electron distribution in such silicon-oxygen compounds plays, especially in the opening of the Si-O-Si bond angle, as well as in the electron distribution over the atoms in the molecule.

In Part I of this series (Schutte and Pretorius 2011) it was reported that the free molecule octahydridosilasequioxane is indeed best described by the symmetry group O_h, but that its symmetry is reduced to that of the site group C_{3i} in the solid state, where the space group is R-3 with Z = 3, as found experimentally (Törnroos 1994) and shown in Figure 1.

It is important to determine just how these symmetries would influence the predicted vibrational spectra and how this relates to the observed infrared spectra (Agaskar 1991; Agaskar and Klemperer 1995). Such results would clear up some unsolved problems in the spectroscopy of silicates, for instance the role of the site group in the solid state and the splitting it induces in degenerate vibrations, as well as the influence of any possible non-rigidity of the molecule. The computational study of Part I, is therefore, extended to include the computed vibrational description of both the free molecule and its counterpart in the solid state.

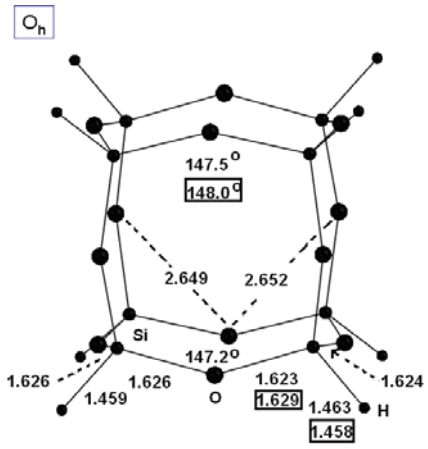

Figure 1: The molecular structure of the octahedral molecule octahydridosilasequioxane as determined in the neutron-diffraction study of Törnroos (1994). The dots at the corners are silicon atoms, the dots in the centre of the edges are oxygen atoms, while the atoms protruding from the corner silicon atoms represent hydrogen atoms. The numbers in squares refer to the computed [G03] Si-O and Si-H interatomic distances. The two crystallographically different Si-O distances are important and should reflect in lifting some degeneracies in the solid-state infrared spectra.

The molecules silane SiH_4, and disiloxane (disilyl ether) SiH_3-O-SiH_3 are used as "reference compounds" in this paper; some of their computed vibrational modes are displayed in Table 1 and compared with corresponding experimental frequencies. We aim to investigate the following vibrational aspects of the octahydridosilasequioxane molecule using advanced computational methods:

1. The molecular vibrational modes of the free molecule, their associated frequencies and relative intensities (in vacuum), comparing them with those of the reference compounds listed above.
2. The computed molecular vibrational modes of the molecule and their associated wave numbers in the solid state.
3. The assignment of the observed IR vibrational bands to specific molecular and solid-state vibrations.

The computational results obtained in this study correlate well with experimental vibrational results. The computational vibrational analysis of octahydridosilasequioxane given here can thus be considered to be representative of silicates in general, and as such contributes to the knowledge of silicate structures and their reactivity in general.

2. Computational approach

All computations on *isolated molecules* were carried out on the SMP architecture of an IBM computer cluster with a pre-compiled set of **GAUSSIAN-03** programs (G03; **Frisch *et al.* 2004**), configured for parallel computing under **POWER LINUX** (SUSE SLES 10.3). Default settings for GAUSSIAN-03 were used as described in the manual (**Frisch & Nielsen 2003**). More details about the computational methodology can be found in **Hirst (1990), Foresman & Frisch (1998)** and **Kohanoff (2006**), as well as in original references cited in the GAUSSIAN manual. All molecular structural and spectroscopic illustrations were done with the program **GAUSSVIEW** (**Dennington *et al.* 2007**), while graphs were drawn with the program **ORIGIN (2006)**. Crystal structure data were visualized from crystallographic information files (CIFs) with the program **MERCURY (2008)** of the Cambridge Crystallographic Data Centre (CCDC).

The default settings of GAUSSIAN G03 were used for all calculations on *free molecules*, except when otherwise indicated. A big basis set was chosen for all computations, namely 6-311++G(3df,3pd), together with the density functional theory (DFT) Beck, three-parameter, Lee–Yang–Parr (B3LYP) exchange correlation functional computational methodology. Optimization computations were done first, followed by frequency calculations in all cases to ensure that the reported structures are determined at potential-energy minima and not at saddle points. No imaginary frequencies for octahedral octahydridosilasequioxane were found in the GAUSSIAN computations.

All *solid state* structural vibrational analysis were carried out on the INTEL architecture of the IBM cluster executing in parallel, using the **MedeA (2011)** set of programs, with special reference to the program **VASP (ver. 5.2.2) (Kresse & Furthmüller 1996 *a*,*b*; Kresse & Joubert 1999)** for crystal structure optimizations and **PHONON (ver. 4.3) MedeA (2011),** for phonon dispersions and phonon densities of states along the special directions of the reciprocal lattice. The software sets available within the MedeA suite **(MedeA 2011)** were used to produce the illustrations from the extensive set of data generated for each run. For the VASP software parameters, the generalized gradient approximation (GGA) Perdue Burke Ernzerhof (PBESol) potential approximation was used on a full structural optimization (relaxed atom positions, cell parameters and cell shape) with projector augmented wave (PAW) plane-wave cut-off of 240 eV, refined as a non-magnetic entity and at an SCF *k*-point spacing of 0.3$Å^{-1}$.

All unit cell frequencies were determined from the spectroscopic unit cell itself using the MedeA/Phonon methodology. Attention is drawn to the existence of two small imaginary phonon modes in the phonon dispersion of the unit cell of octahydridosilsesquioxane. These frequencies were subjected to an intensive computational study, although they do not influence the higher dispersion modes. Since these two small imaginary modes occur in the phonon dispersion when the computation was initiated with the *unrefined experimentally determined unit cell* for each of the basis functions GGA-PBE, GGA-PBEsol, GGA-BLYP and LDA, it was thought that uncertainties in the neutron-diffraction determination might perhaps be the cause. However, the same imaginary modes occur in the phonon dispersion of a fully optimized unit cell, using the same set of basis functions, although the exact frequencies depend upon the specific basis set used, but it never exceeds -25 cm^{-1}.

Imaginary phonon modes usually appear in phonon dispersions where there are problems with the experimentally determined crystal structure (such as wrong space group, wrong cell dimensions, wrong Z, one or more wrong atom fractional coordinates etc.), but such errors should be corrected by the respective refinements in which the atom positions, the cell shape and size, are refined. These refinements, however, does not eliminate the two imaginary modes, which represent harmonic oscillations of the unit cell contents along two lattice directions ("translations"). These two modes should ideally have zero frequencies if the translation modes are cleanly split off from the vibrational modes of the unit cell by the methodology of the computation, and if the rotatory modes are also cleanly split off, as required by the Eckard-Sayvetz conditions (Schutte 1976). Since such problems do not always appear with other compounds, it is thought that these imaginary modes do not arise from inadequate separation of rotation and translation from the internal modes of the unit cell. Another origin of these imaginary frequencies may be found in computational instabilities, which are mainly caused by rounding-off errors of experimental and optimized atomic fractional coordinates and convergence criteria. It is thought that this is the most probable explanation.

3 Molecular vibrational spectra

3.1 Reference molecules: Silane and siloxane

It is important to compare the computed spectra of some reference molecules with the experimental infrared and Raman spectral data, using the same level of theory and the same basis set as used here for octahydridosilasequioxane, thus establishing the validity of the spectral computation. SiH_4(g) and $H_3Si\text{-}O\text{-}SiH_3$ were again chosen for this purpose. For SiH_4(g) the comparison of the experimental data **(Lide 2009, 2010)** and the theoretically computed *unscaled* vibrational data in cm^{-1} are as shown in Table 1. For $H_3Si\text{-}O\text{-}SiH_3$ the experimental values in Table 1 are from **Lord *et al.* (1956); Almenningen *et al*. (1963)** and **Aronson & Lord (1960).**

Attention is drawn to the fact that the assignments and the vibrational mode descriptions for siloxane of the cited authors are not the same as ours, since their assignments are based upon the impossible point group D_{3d}, although the actual point group in such a bent molecule cannot be higher than C_{2v}, which was used in this study. Only the experimental frequencies, which clearly belong to fundamental vibrational modes, are used in the comparison between experimental and theoretically computed frequencies, that is, all overtone and combination modes are ignored:

Table 1: Comparison between the unscaled computed (this work) and experimental vibrational modes (in units of: cm^{-1}) of Silane and Disiloxane, as discussed in the text.
* Lide (2009, 2010)
** Lord et al. (1956), Almenningen et al. (1963) and Aronson & Lord (1960).

	SiH_4 (Silane)			**$H_3Si\text{-}O\text{-}SiH_3$** (Disiloxane)		
Mode notation	Exp. (*)	"G03" Computed (This work)	Diff (%) $\lvert\nu_{exp}-\nu_{calc}\rvert$	Exp. (**)	"G03" Computed (This work)	Diff (%) $\lvert\nu_{exp}-\nu_{calc}\rvert$
Symmetric Si-H stretch	2187	2231	Δ = 44 (2)	2183	2246	Δ = 63 (2)
Anti-Symmetric Si-H stretch	2191	2236	Δ = 45 (2)	2169	2223	Δ = 54 (2)
Symmetric H-Si-H bending (with respect to the 2-fold axis, C_3 axis)	975	981	Δ = 6 (1)	-	-	-
Si-O-Si stretching	--	--	--	1107	1120	Δ = 13 (1)
Anti-Symmetric H-Si-H bending (with respect to the C_2 axis, C_3 axis)	914	923	Δ = 9 (1)	957	971	Δ = 14 (2)
SiH_3 rocking	--	--	--	764	752	Δ = 12 (2)

From these comparisons, it can be concluded that the computational approach used here for compounds containing silicon, hydrogen and oxygen, as well as the geometrical models derived, provide a good approximation to those obtained experimentally; it is especially assuring that no empirical scaling is needed to bring the computed frequencies to agree with the experimental frequencies so that the vibrational modes can be directly identified. The method can thus be applied with confidence to assign the infrared spectra of other similar silicates, and in particular, that of octahydridosilasequioxane, since it is built-up of Si-O-Si units, the structure of which is very similar to that of $H_3Si\text{-}O\text{-}SiH_3$.

The *free* O_h-molecule of octahydridosilasequioxane displays 78 normal modes belonging to the following irreducible representations using group-theoretical methodology (Schutte 1976):

$$\Gamma(\chi) = 3A_{1g} + 1A_{2g} + 4E_g + 3F_{1g} + 6F_{2g} + 3A_{2u} + 3E_u + 6F_{1u} + 4F_{2u}$$

This predicts the occurrence of:

18 *Infrared-active modes* belonging to the F_{1u} representation (6 triply-degenerate infrared bands)

29 *Raman-active modes* belonging to:
$A_{1g}(3)$, $E_g(4)$, $F_{2g}(6)$ representations (generating 13 possible Raman lines)

31 *Inactive modes* belonging to:
$A_{2g}(1)$, $A_{2u}(3)$, $E_u(3)$, $F_{1g}(3)$, $F_{2u}(4)$ representations (occurring in 14 groups)

This is shown diagrammatically in the group-theoretical correlation diagram of Figure 2. Two *site symmetries* of the molecule in the solid state unit cell must be considered, following the arguments given above, namely $C_{3i} = S_6$ *(or* C_i*)*, as well as the non-crystallographic symmetry T_h suggested by Törnroos (1994).

The group-theoretical correlation diagram between these three possibilities and the molecular symmetry group is given in Figure 2. The spectroscopic consequences of this analysis are quite different for the three possible point (or site) symmetries.

From the correlation diagram of Figure 2 it is clear that *site symmetry* C_i is so low that *all* 78 normal modes should be activated in the *solid state* by the lattice perturbation and all the vibrational degeneracies should be lifted. The group-theoretical analysis shows that the three site-group choices may be distinguished as follows:

(i) *The following vibrations should be observed under* C_i :

39 Infrared-active vibrational bands (A_u-symmetry) and
39 Raman-active lines (A_g-symmetry)

(ii) *Under site symmetry* $C_{3i} = S_6$ (or C_i) *there should be*:

13 Raman lines having A_g-symmetry,
13 Raman lines having E_u-symmetry,
13 IR-bands having A_u-symmetry and
13 IR-bands having E_u-symmetry.

(iii) *Under the non-crystallographic point group* T_h*, there should be*:

17 Raman lines altogether (4 A_g, 4 E_g and 9 F_g) and 10 IR-bands of F_u-symmetry.

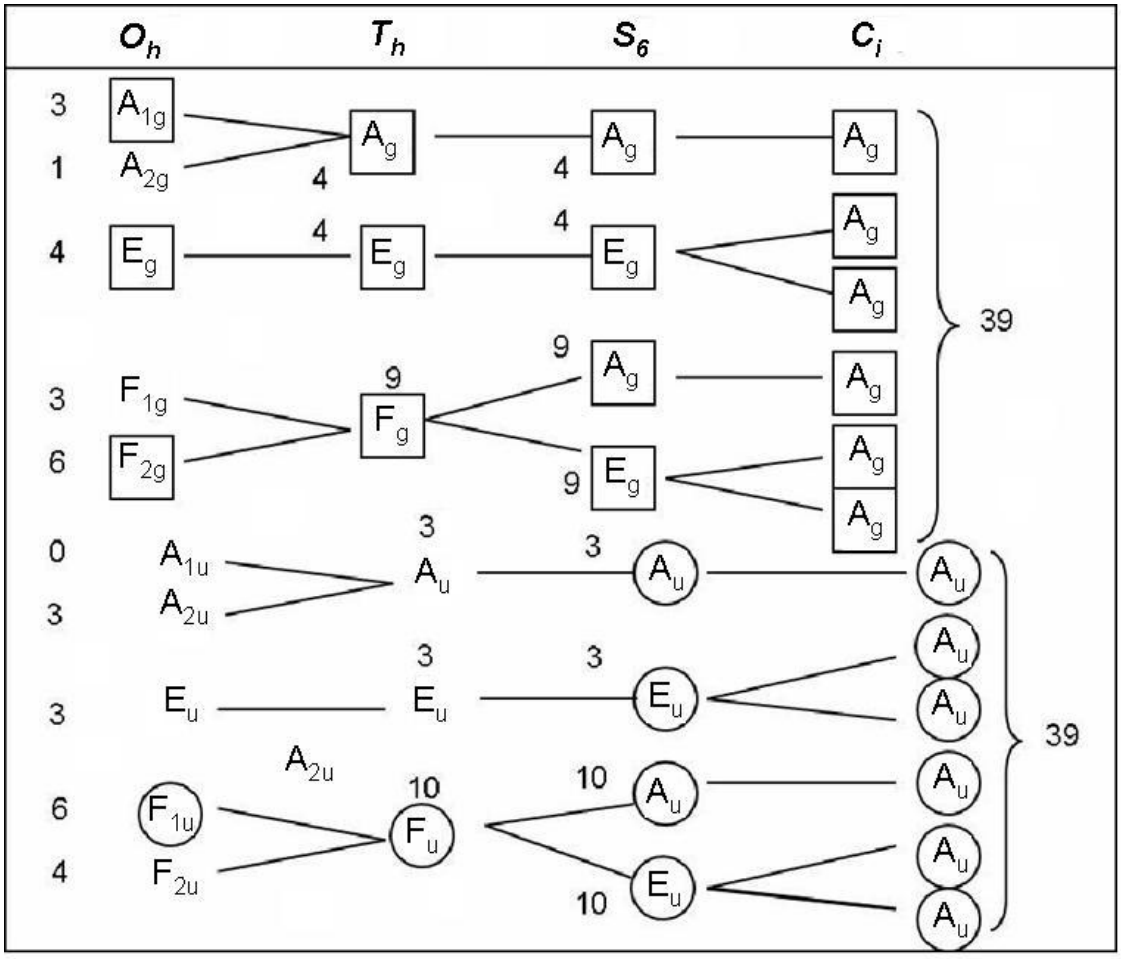

Figure 2: The group-theoretical correlation diagram between the symmetry point group of the free molecule O_h and the two crystallographic site groups ($C_{3i} = S_6$; C_i), as well as the non-crystallographic group T_h discussed in the text. *The point group* T_h *is here formally included because Törnroos (1994) speculated that the symmetry might be* T_h.

In Figure 2 the *ungerade* representations are somewhat offset to the right for the sake of clarity, as well as to emphasize the behavioral differences between the *gerade* (g) and *ungerade* (u) representations and spectroscopic activity. The last two columns are not condensed in the usual way in order to make visualizing of the predicted spectra easier. The symmetry designations of modes, which are Raman active, are designated by a surrounding *square*, while those of the modes, which are infrared active, are surrounded by a *circle*. The number next to each symmetry representation, represents the number of vibration types belonging to that representation; for instance under the column O_h the number six next to the F_{1u} representation, indicates that there are six triply-degenerate infrared active vibrations, which transform like it. The sum of such numbers in each column is equal to the number of normal modes of the molecule (78), when degeneracies are taken into account. The number of IR-active, Raman-active and inactive bands in the predicted spectra of the molecule can easily be determined under each one of the four point groups listed.

Table 2 displays the band wave numbers of the experimentally-obtained *Nujol* IR-spectra (Agaskar *et al.* 1991,1995) of *solid* octahydridosilasequioxane (column 2) and the G03 computed wave numbers of the infrared active modes of the *free molecule* (column 3), as well as the G03 computed Raman spectra (column 4) and the optically inactive modes (column 5). It is seen that there is very little difference between the experimental and computed IR active vibrational wave numbers (columns 2, 3 and 6).

The GAUSSIAN G03 computation thus allows a complete and unambiguous assignment of all the vibrational modes responsible for the infrared spectrum of the solid state. These normal modes were also computed and some of them are displayed in Figures 4 to 6 and also include some Raman-active modes, which are important for discussions below. The nature of these modes is discussed in the respective legends of the figures. It is to be noted that although the Si-H stretching modes are almost pure stretches, some of them have very small contributions from the motions of the Si-atoms. Most of the Si-H bending normal modes show very little coupling with other internal coordinates, such as the Si-O-Si bending modes (Figure 6).

The assignment of the *experimentally-recorded IR spectra* of Agaskar *et al.* (1991, 1995) of the solid compound shown in Table 2, shows that the degeneracies of the doubly and triply degenerate vibrations of the octahedral molecule octahydridosilasequioxane are *apparently not lifted* (no indication of band-splitting) and that no inactive modes are activated, although it must be pointed out that such *Nujol* spectra display rather broad bands, which do not easily provide evidence for band splitting. However, there is no sign in the *IR spectrum* that any (or all) of the inactive molecular vibrations are activated by the possible reduction of the molecular symmetry from fully octahedral to only inversion symmetry. *This means that the perturbation, which the molecule experiences by the crystalline field, is negligently small when placed in these crystalline fields of* $C_{3i} = S_6$ *(or* C_i*) site symmetry, so that the molecule behaves as if it were octahedral.* The same applies to the non-crystallographic point group T_h, since the IR-spectrum shows no sign of the 4 F_{2u} modes, which should be activated under T_h.

This conclusion is reinforced by the splittings computed in the phonon dispersion (Table 2, column 6), which are very small, for example in the highest Si-H stretch it is about 10 – 20 wave numbers. It is clear that such small splitting cannot be resolved at room temperature in a *Nujol* mull and even molecular spectra recorded at about 4 K will hardly resolve it into separate components. This means either that the crystalline field acting upon the molecule is small or that the two independent crystal structure determinations cited above yielding the same space group and molecular structure, must both be erroneous. It is to be noted that the phonon dispersion calculation of PHONON delivers 3N = 84 unit cell modes; the six modes not belonging to the (3N-6) internal vibrational modes of the unit cell, are therefore, not listed in Table 2.

The possibility that the crystal structure was wrongly determined must be very small, because the orthorhombic unit cell parameters of the trigonal lattice are very definite and can hardly be confused with those of a cubic cell in which the site symmetry of the molecule is octahedral. It therefore, seems possible that the nature of the crystal field H' is such that the perturbation λH it

exerts on the vibrational Hamiltonian H of the octahedral molecules is small, so that $H` = H + \lambda H$ is not very different from H. This is borne out by the very small differences in the Si-O bond distances in the crystal discussed above: they are just outside the experimental error on these bond lengths.

3.2 Normal modes of octahydridosilasequioxane

In order to describe the 78 normal modes of the octahydridosilasequioxane molecule in a simplified way, a symbolic cube is constructed as shown in Figure 3. The symbolic cube that represents the atom planes of the isolated octahedral octahydridosilasequioxane molecule passing either through the H-atoms, or the Si-atoms or the O-atoms, as the case may be. The right-handed coordinate system is placed in the molecule on the centre of mass. The sides of the cube are numbered as shown in order to briefly describe some of the normal modes of vibration of the molecule. For instance, vibrational mode 75 shown in Figure 4 and Figure 5e is one of the F_{1u} anti-symmetric Si-H stretching modes and the two sets of participating H-atoms that stretch out of phase, are placed on A and C sides, respectively, those on A moving radially outwards and those on C radially inwards at the same time.

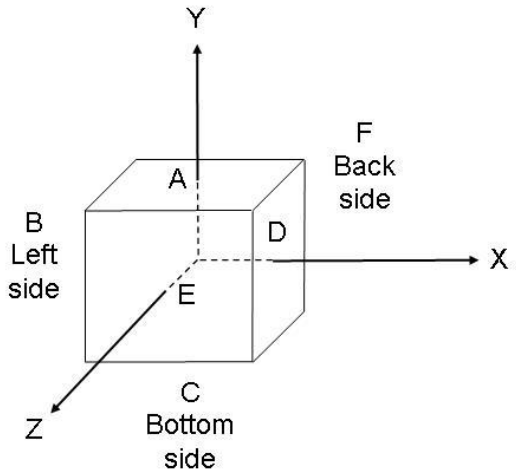

Figure 3: The symbolic cube that represents the atom planes of the isolated octahedral octahydridosilasequioxane molecule passing either through the H-atoms, or the Si-atoms or the O-atoms, as the case may be.

The computed IR and Raman spectra for the free octahydridosilasequioxane molecule are shown in Figure 4. It is clear that the spectra show a paucity of active vibrations for such a large molecule. This is due to the fact that most of the vibrational transitions show very low transition probabilities and hence, very low intensities. In addition, there are very many spectroscopically inactive modes that do not couple with electromagnetic radiation, as discussed above. The numbers on Figure 4 refer to the numbers of the vibrational modes, which are listed in inverse order (from the highest, Nr. 78, to the lowest, Nr. 1) in Table 2. Only one member of each degenerate set of normal modes is shown in Figure 4 and in Table 2. In the following Figures (5 & 6) the normal modes of some of the most important active vibrations are shown and briefly described.

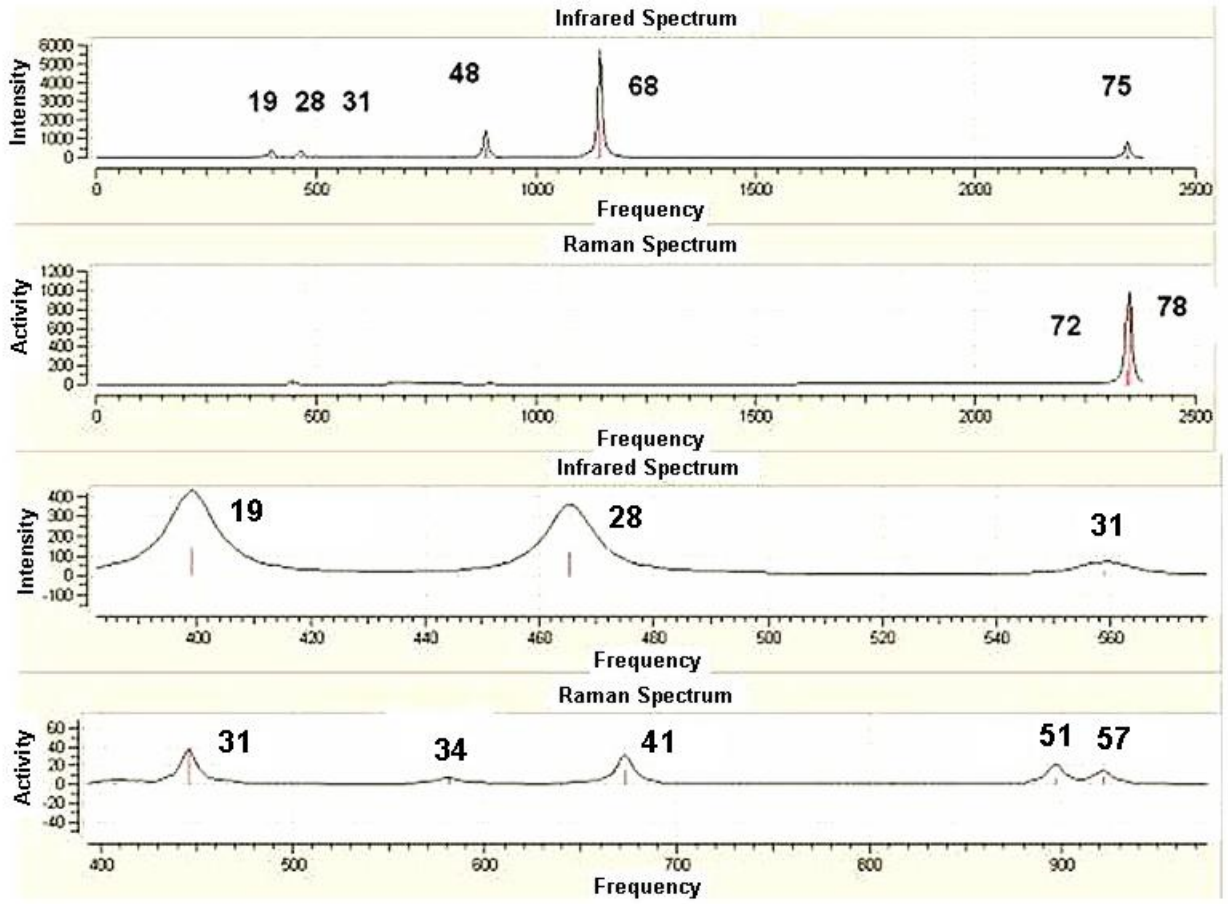

Figure 4: The G03 computed infrared (IR) and Raman spectra of the octahedral octahydridosilasequioxane molecule. In the lower part a severely enlarged view of parts of the spectra is shown in order to bring out some of the small bands; it must be noted that the both the ordinate and abscissa scales differ in the illustrations. Note: *The low intensity bands (second curve) are not marked in this Figure, but they are listed in Table 2.*

The computed Raman-active anti-symmetric Si-H stretching mode (number 78) at 2351 cm^{-1} (Figure 5f) as well as (numbers 72 - 74) at 2342 cm^{-1} (Figure 5d) and the IR-active totally symmetric Si-H stretching modes (numbers 75 - 77) at 2345 cm^{-1} (Figure 5e), in the computed IR and Raman spectra (enlarged) in Figure 4, depict almost pure Si-H stretching modes. In these modes the amplitude of the H-atoms is much larger than that of the Si-atoms, with very little interaction with bending and other modes, including the Si-O stretches. This is confirmed by the phonon density of states for the upper part of the phonon dispersion graphs. The H-atoms move in phase along the diagonal lines of the cube of Figure 3.

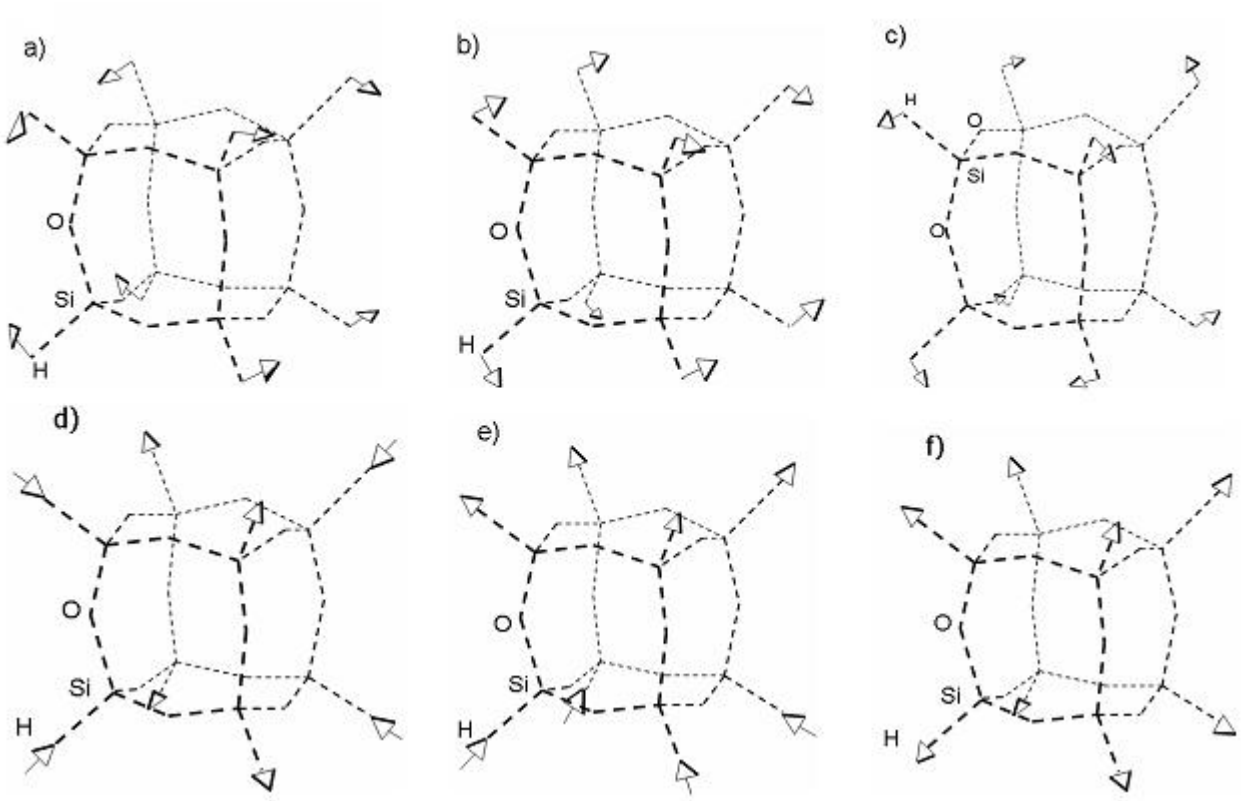

Figure 5: Raman (symmetric) and Infra-red (asymmetric) active Si-H stretching and deformation (wagging) modes. Mode numbers (below) refer to the molecular frequency assignments represented in Figure 4.

a) Symmetric Si-H wag.	Mode 41-42 at 673 cm^{-1}, symmetry E_g,	Raman active
b) Asymmetric Si-H wag.	Mode 48-50 at 886 cm^{-1}, symmetry F_{1u},	Infra-red active
c) Symmetric Si-H wag.	Mode 51-53 at 896 cm^{-1}, symmetry F_{2g},	Raman active
d) Symmetric Si-H stretch.	Mode 72-74 at 2343 cm^{-1}, symmetry F_{2g},	Raman active
e) Asymmetric Si-H stretch.	Mode 75-77 at 2345 cm^{-1}, symmetry F_{1u},	Infra-red active
f) Symmetric Si-H stretch.	Mode 78 at 2351 cm^{-1}, symmetry A_{1g},	Raman active

Mode 78 shown in Figure 5f is the Raman active Si-H stretching normal mode A_{1g}, in which the (A, C) plane H-atoms are moving radially outwards and the Si-atoms radially inwards in phase with the H-atoms. The amplitudes of the Si-atoms are far too small to show up on the scale of this Figure. This mode does not change when described with respect to the (B, D) or (E, F)-planes, since it is invariant to all the symmetry operators of the point group O_h.

For the anti-symmetric Si-H stretching modes 75 to 77 (Figure 5e), the amplitude of the Si-atoms is so small that the motion vectors cannot be displayed. The radial inward motion of the lower circle of H-atoms is balanced by a small radial outward motion of the Si atoms; the reverse is true for the motions of the upper ring Si and H atoms.

Figure 5d shows the symmetric Si-H stretch (symmetric with respect to the centre of inversion). The motion of four hydrogen atoms is radially outwards on the one diagonal plane that passes through them and that of the other four is radially inwards on the other diagonal plane that is perpendicular to the other two. The other two modes of this triply degenerate set are along the other two pairs of perpendicular diagonal planes of the cube (Figure 3).

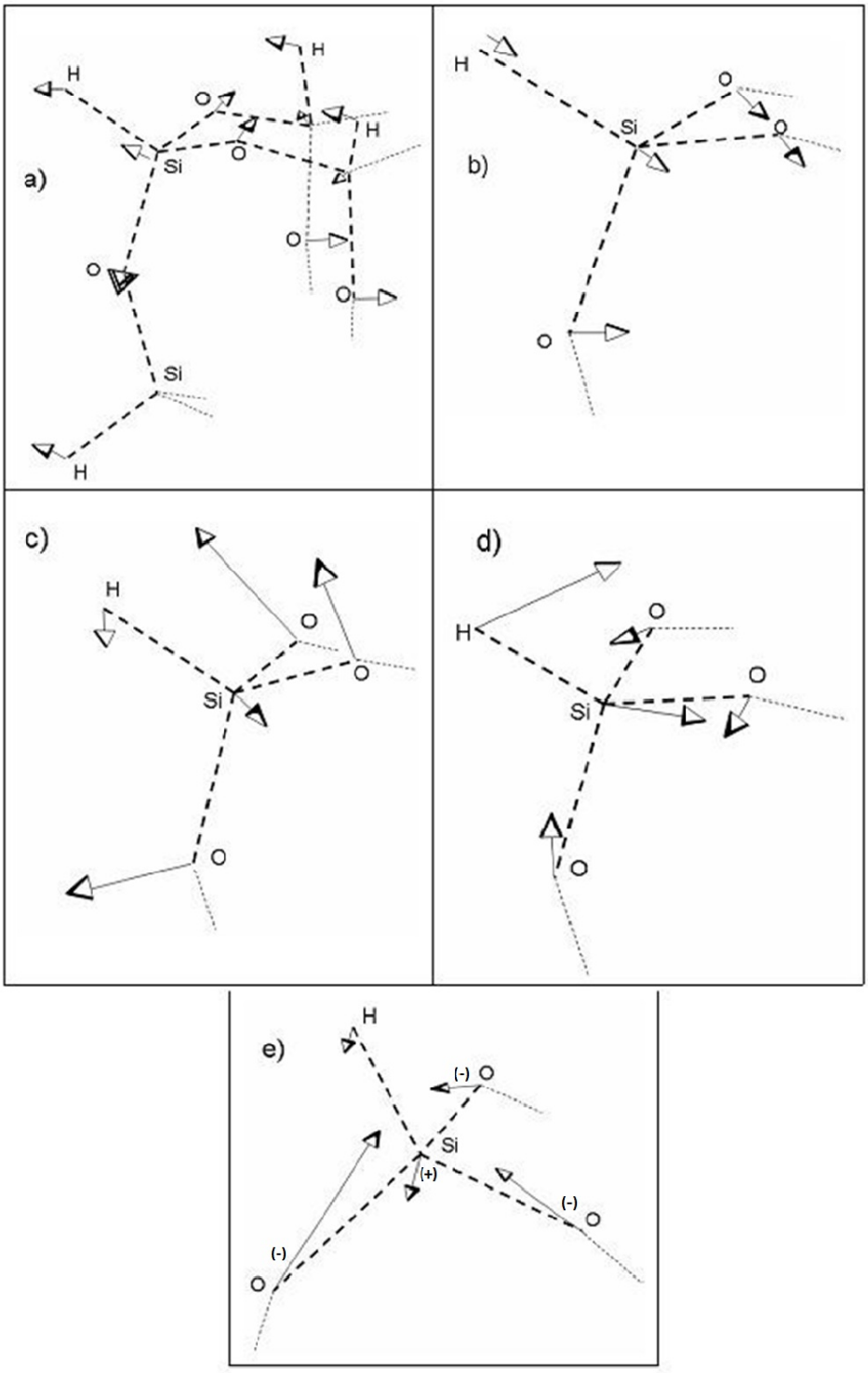

Figure 6: Raman (symmetric) and Infra-red (asymmetric) active cage deformation modes. Mode numbers (below) refer to the molecular frequency assignments represented in Figure 4.

a) Asymmetric O-Si-H twist	Mode 19-21 at 399 cm^{-1}, symmetry F_{1u}, Infra-red active
b) Cage breathing	Mode 27 at 446 cm^{-1}, symmetry A_{1g}, Raman active
c) Asymmetric Si-O-Si bend	Mode 28-30 at 465 cm^{-1}, symmetry F_{1u}, Infra-red active
d) H-Si …Si-H torsion	Mode 31-33 at 558 cm^{-1}, symmetry F_{1u}, Infra-red active
e) Asymmetric Si=O stretch	Mode 68-70 at 1146 cm^{-1}, symmetry F_{1u}, Infra-red active

Figure 6e shows an enlargement of the lower part of the molecule for mode 68. A (+) sign next to a Si-atom denotes that the atom is displaced perpendicularly upwards, while a (-) sign next to the arrow emanating from an oxygen atom is pointing slightly downwards. There are two Si atoms that do not move during the normal mode. The amplitude of motion of the Si and O atoms during the execution of this mode is much smaller than that of the hydrogen stretching modes due to the mass effect and to the fact that at least 8 bonds, each with its own force constant are involved when the atoms in the Si-O-Si group move.

Figures 5b and 6e display the two infrared active triply-degenerate anti-symmetric O-Si-H bending modes of numbers 48 - 50 at 886 cm^{-1} and numbers 68-70 at 1146 cm^{-1} respectively. The Si-H-bending mode of modes 48 - 50 is almost pure H-atom bending modes and show little indication of coupling with Si-atom and O-atom movements. However, the motion of the H-atom is heavily coupled with those of the O-atoms in modes 68 – 70 (Figure 6e).

Figure 5b shows that the triply degenerate F_{1u} mode 48 can be described as a hydrogen atom wagging movement involving the four hydrogen atoms in the A and C planes of the cube (Figure 3); the other two members are the wagging motions of the hydrogen atoms of the (B, D) and (E, F) planes, respectively. This wagging motion takes place almost without involving the Si and the O atoms. The weak E_g Raman band at 921 cm^{-1} is due to a doubly degenerate normal mode (mode 57) which is very similar to that of mode 48. The triply degenerate F_{2g} mode 51, which occurs in the computed Raman spectrum at 896 cm^{-1} (Figure 5c), can be described as a symmetric H-Si-O-Si-H bending mode, involving the four hydrogen atoms (A, C), (B, D) and (E, F) planes, respectively, in which the pair of Si-H bonds bend out of phase with a rather large amplitude. This mode is symmetric with respect to the centre of inversion, as well as to a rotation about a two-fold axis.

The triply degenerate infrared anti-symmetric Si-H-bending mode (numbers 28 - 30) at 465 cm^{-1} is shown in Figure 6c. In contrast with the Si-H-bending modes of Figures 5b & 6e, this Si-H bending mode shows strong coupling with the Si-O-Si bending motion in which some O-atoms move inwards and other outwards; there is almost no Si-atom motion discernible. Another triply degenerate infrared Si-O-Si bending mode is shown for mode numbers 19 – 21 occurring at 399 cm^{-1} (Figure 6a). This mode couples with the OH-bending motions to some extent and does involve Si-atoms to a small extend. The triply degenerate anti-symmetric infrared active set of modes (31 - 33) occurring at 558 cm^{-1} (Figure 6d*)* shows strong coupling with Si-atom motions, but not with O-atoms.

The three totally symmetric Raman active modes are shown in Figure 6b (cage breathing). Mode 27 occurs at 445 cm^{-1} and is a symmetric Si-H stretching mode, but heavily coupled with the O-atom movement in a symmetric Si-O-Si bending mode. Normal modes 41 - 42, which occur at 672 cm^{-1} (Figure 5a) are totally symmetric doubly degenerate Raman modes, displaying the Si-O-H bending modes with almost no O and Si involvement. Modes 51-53, which occur at 896 cm^{-1} (Figure 5c) are also totally symmetric triply degenerate O-Si-H bending modes, again with very little Si and O-atom involvement. The other Raman modes are so weak that they will hardly be observable and are not displayed here; the inactive infrared and Raman modes are also not displayed (see table 2).

3.3 Phonon dispersion and densities of states

The theoretical computation of the vibrational modes and their respective symmetries for compounds consisting of molecules and/or ions imbedded in the crystal field in the solid state is very important. These results can be used to predict the Raman and infrared spectra of compounds; this is especially important for the understanding of phase transitions in which the symmetry changes and for determining the splitting of degenerate vibrations, as well as the splitting due to intermolecular vibrational coupling. The symmetry of the *unit cell* plays an important role in

this analysis, but care has to be taken not to indiscriminately compute vibrations in a crystallographic unit cell (which can contain Z(3*N*) degrees of freedom, where, *Z* is the number of molecules in the unit cell and *N* the number of atoms in a molecule), but to use the *spectroscopic unit cell*. The relevant theory is found in Adams and Newton (1970A), Adams and Newton (1970), Fately, McDevitt and Bentley (1971), Bertie and Bell (1970), Bertie and Kopelman (1971), Schutte (1973) and Hahn (2005) and references therein.

The spectroscopic unit cell is identical to the crystallographic unit cell in the case of the space groups of which the crystallographic symbol starts with a *P*, so that the spectrographic unit cell in this case is identical with the *Bravais cell*. For those space groups starting with the *B*, *C*, *I* and *F*-symbols, the crystallographic unit cell contains, respectively, 2, 2, 3, and 4 spectroscopic or Bravais unit cells. However, the unit cell of octahidridosequisiloxane belongs to the rhombohedral class, where the spectroscopic unit cell can be either identical to the crystal unit cell, or one-third of it. Since the unit cell in this case is described by the symbol *R*-3, with Z = 3, it is clear that the spectroscopic unit cell to use for the calculation of the phonon frequencies, contains only one molecule. This means that there will be 84 phonon modes, of which the six lowest will not be molecular, but crystal modes. The (3*N*-6) = 78 *crystal phonon frequencies* are listed in Table 2.

The 78 phonon frequencies and their spectroscopic activities should thus have their counterparts in the experimental IR and Raman spectra of the solid state. This means that a comparison between the observed IR frequencies and the theoretically calculated spectrum should thus help to identify the molecular symmetry in the solid state. In addition, any splitting of the F-molecular modes of the free ion in the crystal into (*A* + *E*) modes should thus be an indication of the symmetry (C_{3i} = S_6) and strength of the crystalline field in which the molecule is imbedded. There should be no further splitting of the *A*, *E* and *F*-modes due to intermolecular vibrational coupling, since there is only one molecule in the spectroscopic unit cell.

The MedeA-Phonon computation shows that the top band of the optical phonon modes of solid octahydridosilasequioxane occurs as four clearly separated band regions in the *dispersion curves* as measured at the Γ-point of the reciprocal cell (Figure 7 at the top and enlarged in Figure 8). This band shows the following number of components upon enlarging (reading from the top line downwards): 2,1,2,3. According to the phonon density of states (Figure 7 at the right) this group of curves clearly belongs to the motion of the H-atoms, with very small components of Si movement. These 4 band regions thus belong to the Si-H stretching modes of the spectroscopic *unit cell*. According to Figure 8 there are in total 8 Si-H stretching modes. The group-theoretical assignment of these modes as obtained from the PHONON analysis is also indicated in Figure 8. The *u* and *g* triply-degenerate *F*-modes of the free O_h-molecule are split into *A* and *E* modes in the unit cell with unit cell symmetry C_{3i}. The perturbing crystalline field λH of symmetry C_{3i} = S_6 is so small that the *A* and *E* components of the *F*-modes are split by only 20 cm^{-1} for the u-case and by 10 cm^{-1} for the g-case as can be seen from Figure 8 and Table 2; as said above, this splitting is far too small to show up in any *Nujol*-based IR spectrum. This A and E-mode splitting pattern for the F-modes is also followed by the other F-modes as displayed in Table 2.

The *Gaussian computation* for the *free octahedral molecule* displayed in Table 2 shows that there are 8 normal modes in the Si-H stretching region with degeneracies 1 (A_{1g}), 3 (F_{1u}), 3 (F_{2g}), 1 (A_{2u}) (reading downwards from the highest wave number), of which the latter is inactive in both the IR and in the Raman. If the site symmetry of the molecule is indeed C_i, then the degeneracy of the modes will be totally lifted, and their symmetry should be reduced into either an A_g or an A_u mode (see Figure 2). The discussion in the previous paragraph, combined with the data displayed in Figures 2 and 7, clearly eliminate the assignment of the site group C_i for the molecule. The same data also eliminate the point group T_h suggested by Törnroos (1994).

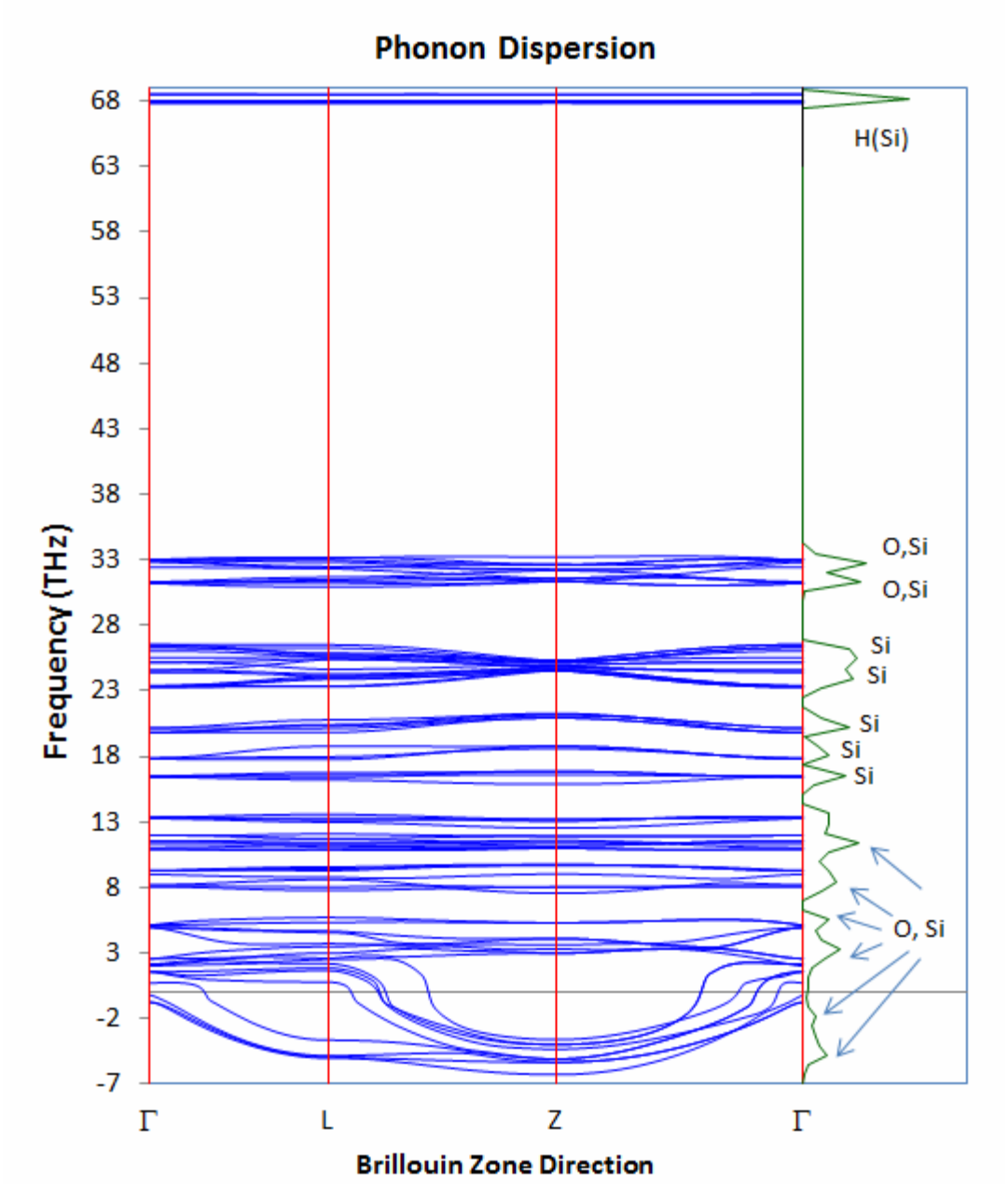

Figure 7: The phonon dispersion of the optimized unit cell of octahydridosilasequioxane (left) and the phonon total density of states, showing the involvement of the individual atoms in the molecular modes and phonon dispersion.

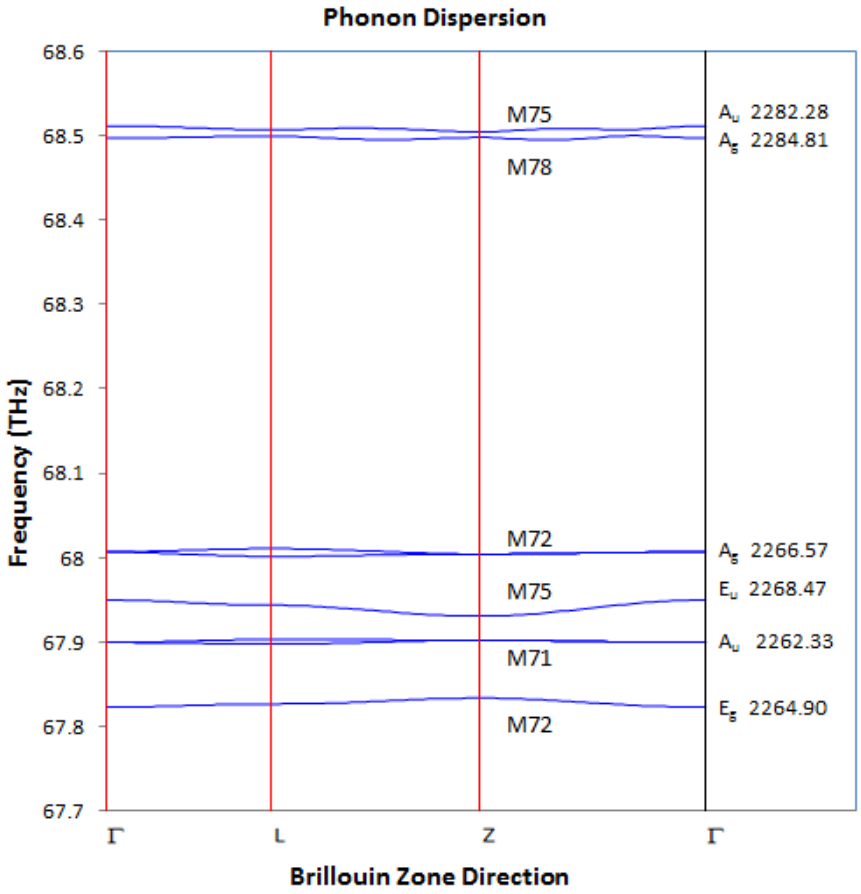

Figure 8: The top band of the optical phonon modes of solid octahydridosilasequioxane (Figure 7), shown as the eight Si-H stretching modes. Respective mode numbers (refer Table 2, Col. 1) are shown as well.

4 Conclusions

The results of this computational study allow us to reach the following conclusions, which are not only important for octahydridosilasequioxane, but also for silicate structures in general:

1. The all-electron GAUSSIAN G03 computed structure of the optimized free molecule confirms that it can be described by the molecular point group O_h, as shown in Figure 1.
2. The computed optimized geometrical O_h structure of the free molecule octahydridosilasequioxane is very near to that determined crystallographically by Törnroos (1994), except that the crystal is somewhat distorted in the unit cell by packing forces (the origin of which is discussed below), reducing the site symmetry to C_{3i} = S_6. Attention is especially drawn to the fact that there are two different Si-O bond lengths in the crystal emanating from the same silicon atom. The difference between the bond lengths is larger than the least-squares error of the bond-length determination of Törnroos (1994) and might be attributed to the novel packing situation of the molecules in the crystal as discussed in Part I of this series (Schutte and Pretorius 2011).
3. A full normal coordinate analysis was done on the free molecule octahydridosilasequioxane, as well as a theoretical computation of all the 78 normal modes of vibration of the molecule

and their associated frequencies. This allowed us to assign all the IR active vibrational modes of a *Nujol* mull as reported by Agaskar (1991) and to conclude that the crystal packing forces do not cause measurable shifts in the vibrational frequencies. These forces, although they are large enough to contribute to the crystal packing, are not so large that they contribute to the unit cell couplings, although there is some A, E mode splitting for the F-modes. In the crystal in any case, *Nujol* spectra are usually so broad that small splitting in degenerate modes cannot be observed nor can the occurrence of small frequency shifts be identified.

4. The MedeA-PHONON computation of the phonon modes of the crystal of octahydridosilasequioxane and the corresponding densities of states confirm the conclusions reached in the previous point. They furthermore allow us to identify all the IR, Raman and inactive vibrational modes. It would be interesting to compare the results of any future Raman study with the theoretically computed solid-state modes we report here.

REFERENCES

Adams, D.M. and Newton, D.C. 1970 Tables for Factor-group Analysis of the Vibrational Spectra of Solids. J. Chem. Soc **A**., 2822.

Adams, D.M. and Newton, D.C. 1970 Tables for Factor Group Analysis, Beckmann RIIC Ltd., Croydon.

Agaskar, P. A. 1991 New synthetic route to the hydridospherosiloxanes O_h-H8Si8O12 and D_{5h}-H10Si10O15. *Inorg. Chem.* **30**, 2707–2708. (doi:10.1021/ic00013a002)

Agaskar, P. A. & Klemperer, W. 1995 The higher hydridospherosiloxanes: synthesis and structures of $H_nSi_nO1.5_n$, (*n* =12, 14, 16, 18). *Inorg. Chim. Acta* **229**,355–364. (doi:10.1016/ 0020-1693(94)04266-X)

Almenningen, A., Bastiansen, O., Ewing, V., Hedberg, K. & Traetteberg, M. 1963 The molecular structure of disiloxane, $(SiH_3)_{2O}$. *Acta Chem. Scand*. **17**, 2455–2460. (doi:10.3891/acta.chem.scand.17-2455)

Aronson, J. R., Lord, R. C. & Robinson, D. W. 1960 Far infrared spectrum and structure of disiloxane. *J. Chem. Phys.* **33**, 1004–1007. (doi.org/10.1063/1.1731323)

Bertie J.E. and Bell, J.W. 1971 Unit cell group and Factor group in the theory of the electronic and vibrational spectra of crystals, J. Chem. Phys. **54**, 3613,160.

Bertie J.E. and Kopelman, R. 1971 On the unit cell group and Factor group in the theory of the electronic and vibrational spectra of crystals, J. Chem. Phys. **55**, 3613.

Birchall, J. D. & Chappell, J. S. 1988 The chemistry of aluminium and silicon in relation to Alzheimer's disease. *Clin. Chem.* **34**, 265–267.

Bilinski, H., Horvath, L. & Trbojevic-Cepe, M. 1992 Precipitation and characterization of an aluminosilicate from AlCl3–Na2SiO3–HCl in serum, of interest for Alzheimer disease. *Clin. Chem.* **38**, 2019–2024.

Fateley, W.G. McDevitt N.T. and Bentley, F.M. 1971 Infrared and Raman selection rules for lattice vibrations: The correlation method, Appl. Spectry. 25,155.

GaussView: **Version 4.1** 2007 Dennington R.(II), Keith T. and Millam J., *Semichem, Inc., Shawnee Mission, KS*.

Gaussian 03: **Revision C.02**, 2004 Frisch M.J., Trucks G.W., Schlegel H.B., Scuseria G.E., Robb M.A., Cheeseman J.R., Montgomery J.A. Jr., Vreven T., Kudin K.N., Burant J.C., Millam J. M., Iyengar S.S., Tomasi J., Barone V., Mennucci B., Cossi M., Scalmani G., Rega N., Petersson G.A., Nakatsuji H., Hada M., Ehara M., Toyota K., Fukuda R., Hasegawa J., Ishida M., Nakajima T., Honda Y., Kitao O., Nakai H., Klene M., Li X., J, Knox. E., Hratchian H.P., Cross J.B., Bakken V., Adamo C., Jaramillo J., Gomperts R., Stratmann R.E., Yazyev O., Austin A.J., Cammi R., Pomelli C., Ochterski J.W., Ayala P.Y., Morokuma K., Voth G.A., Salvador P., Dannenberg J.J., Zakrzewski V.G., Dapprich S., Daniels A.D., Strain M.C., Farkas O., Malick D.K., Rabuck A.D., Raghavachari K., Foresman J.B., Ortiz J.V., Cui Q., Baboul A.G., Clifford S., Cioslowski J., Stefanov B.B., Liu G., Liashenko A., Piskorz P., Komaromi I., Martin R.L., Fox D.J., Keith T., Al-Laham M.A., Peng C.Y., Nanayakkara A., Challacombe M., Gill P.M.W., Johnson B., Chen W., Wong M.W., Gonzalez C. and Pople J.A. *Gaussian, Inc., Wallingford CT*. (http://www.gaussian.com).

Hahn (Editor), T. 2005 International Tables for Crystallography, Fifth Edition, Springer, Berlin.

Lord, R. C., Robinson, D. W. & Schumb,W. C. 1956 Vibrational spectra and structure of disiloxane and disiloxane-d16. *J. Am. Chem. Soc.* **78**, 1327–1332. (doi:10.1021/ja01588a018)

MedeA 2011 *PHONON software version 4.30*. Copyright Prof. K. Parlinski. See K. Parlinski, Software Phonon. See http://wolf.ifj.edu.pl/phonon/.

MedeA 2011 *Materials design and exploration analysis software*. Materials Design, Inc., v. 2.7.2

MedeA User's Guide, version 2.4. *Theoretical background* at the licensed software product web-site: http://www.materialsdesign.com

Schutte, C. J. H. 1976 The theory of molecular spectroscopy. In *The quantum mechanics and group theory of vibrating and rotating molecules*, vol. 1. Amsterdam, The Netherlands: North-Holland.

Seddon, D. 2006 Gas usage and value: the technology and economics of natural gas use in the process industries. Tulsa, OK: Penwell Publishers.

Schutte C.J.H. & Pretorius J.A. 2011 A computational study of the molecular and crystal structure and selected physical properties of octahydridosilasequioxane–$(Si_2O_3H_2)_4$. I. Electronic and structural aspects. *Proc. R. Soc. A* 467:928-953 (Published online before print, October 27, 2010, doi:10.1098/rspa.2010.0388)

Schutte, C.J.H. 1973 Topics in Current Chemistry, The infra-red spectra of crystalline solids, **36**, 57.

SUSE LINUX. 2009 Enterprise SERVER (SLES) Computer operating system, v. 10.3. An OPEN SUSE computer software project sponsored by Novell, Inc., USA.

Törnroos, K. W. 1994 Octahydridosilasesquioxane determined by neutron diffraction. *Acta Crystallogr.* **C50**, 1646–1648. (doi:10.1107/S0108270194005342)

Vora, B. V., Marker, T. L., Barger, P. T., Nilsen, H. R., Kvisle, S. & Fuglerud, T. 1997 Economic route for natural gas conversion to ethylene and propylene. *Stud. Surf. Sci. Catal.* **107**, 87–98. (doi:10.1016/S0167-2991(97)80321-7)

Wilson, S. & Barger, P. 1999 The characteristics of SAPO-34 which influence the conversion of methanol to light olefins. *Micropor. Mesopor. Mater.* **29**, 117–126. (doi:10.1016/S1387-1811 (98)00325-4)

Table 2: The (3N-6) = 78 vibrational mode numbers (column 1) of the free O_h-molecule and their respective symmetries, the experimental wave numbers (column 2, Agaskar and Klemperer 1995), the computed G03 wave numbers of this study and their relative intensities (columns 3 - 5; their respective symmetries are found in column 1). The numbers in brackets after the computed wave numbers refer to the relative computed intensity of the band. The six phonon modes at 52.47 E_g(R), 24.15 A_g(R), -24.95 A_u(IR) and -5.77 cm^{-1} E_u(IR) (derived from the GGA-PBEsol functional under VASP), are not listed in column 7; they do not belong to the *vibrational modes* of the unit cell, but to rotations and translations (having *g* and *u* symmetry under S_6, respectively). The vibrational symmetry descriptions derived for the solid state are listed in column 6, while the respective frequencies for the basis functionals GGA-PBEsol and GGA-BLYP (VASP) are found in columns 7 and 8.

G03 mode numbers, O_h symmetry	**Exp. IR (Nujol) cm^{-1}** (Agaskar and Klemperer 1995)	**G03 Computed, IR, cm^{-1} O_h symmetry** (This work)	**G03 Computed, Raman, cm^{-1} O_h Symmetry** (This work)	**G03 Computed, Inactive cm^{-1} O_h symmetry** (This work)	**Phonon symmetry** Activity: (R or IR) (This work)	**Computed phonon, cm^{-1} (S_{6i}) PBEsol (VASP 5.2.2)** (This work)	**Computed phonon, cm^{-1} (S_{6i}) BLYP (VASP 5.2.2)** (This work)
78 A_{1g}	-	-	2351.39 (884)	-	A_g R	2 284.81	2 359.46
75, 76, 77 F_{1u}	2290 (s)	2345.51 (302)	-	-	A_u IR E_u IR	2 285.28 2 268.47	2 359.53 2 336.95
72, 73, 74 F_{2g}	-	-	2342.93 (155)	-	A_g R E_g R	2 266.57 2 264.90	2 345.69 2 330.91
71 A_{2u}	-	-	-	2341.29 (0)	A_u IR	2 262.33	2 332.71
68, 69, 70 F_{1u}	1140(vs)	1146.10 (1953)	-	-	A_u IR E_u IR	1 087.76 1 100.26	1 077.01 1 075.58
65, 66, 67 F_{2g}	-	-	1137.28 (2)	-	E_g R A_g R	1 101.26 1 094.72	1 079.01 1 072.34
64 A_{2u}	-	-	-	1113.09 (0)	A_u IR	1 081.98	1 063.77
61, 62, 63 F_{1g}	-	-	-	1050.50 (0)	A_g R E_g R	1 045.56 1 041.45	1 024.17 1 019.50
59, 60 E_u 57, 58 E_g	- 918 (w)	- -	- 921.40 (7)	1049.90 (0) -	E_u IR E_g R	1 042.15 885.38	1 020.84 915.73
54, 55, 56 F_{2u}	-	-	-	914.77 (0)	E_u IR A_u IR	878.07 869.00	907.99 895.39
51, 52, 53 F_{2g}	-	-	896.89 (7)	-	A_g R E_g R	851.72 840.35	885.61 871.20
48, 49, 50 F_{1u}	870 (s) 815 (sh)	886.06 (504)	-	-	E_u IR A_u IR	820.30 814.30	850.25 843.68
46, 47 E_u	-	-	-	812.55 (0)	E_u IR	779.91	799.22
43, 44, 45 F_{1g}	-	-	-	811.06 (0)	A_g R E_g R	780.64 776.77	799.49 797.02
41, 42 E_g	-	-	672.94 (16)	-	E_g R	673.70	669.53
38, 39, 40 F_{2u}	-	-	-	662.68 (0)	E_u IR A_u IR	662.32 661.32	656.35 652.62

35, 36, 37 F_{2g}	-	-	596.59 (0.2)	-	A_g R E_g R	597.38 594.01	590.61 583.44
34 A_{1g}	-	-	581.05 (8)	-	A_g R	550.81	567.93
31, 32 33 F_{1u}	500 (sh)	558.91 (24)	-	-	A_u IR E_u IR	549.55 548.71	551.21 545.24
28, 29, 30 F_{1u}	470 (w)	465.38 (121)	-	-	E_u IR A_u IR	445.57 442.71	449.38 448.54
27 A_{1g} 25, 26 E_g	- -	- -	445.90 (37) 422.80 (0.35)	-	A_g R E_g R	445.11 400.11	442.51 411.05
22, 23, 24 F_{2g}	-	-	407.65 (1.5)	-	E_g R A_g R	387.57 378.66	392.54 389.44
19, 20, 21 F_{1u}	395 (m)	399.16 (143)	-	-	A_u IR E_u IR	368.52 364.95	378.39 374.76
16, 17, 18 F_{1g}	-	-	-	332.08 (0)	A_g R E_g R	310.51 309.95	319.89 319.32
15 A_{2u}	-	-	-	317.99 (0)	A_u IR	300.74	306.25
12, 13, 14 F_{2u}	-	-	-	292.00 (0)	A_u IR E_u IR	274.32 269.82	282.93 279.69
9, 10, 11 F_{2g}	-	-	170.06 (2)	-	A_g R E_g R	164.68 167.12	170.62 168.15
7, 8 E_u 5, 6 E_g	- -	- -	- 72.48 (0.04)	161.81 (0) -	E_u IR E_g R	72.15 86.13	172.89 103.27
2, 3, 4 F_{2u}	-	-	-	59.61 (0)	A_u IR E_u IR	67.58 72.15	88.03 92.26
1 A_{2g}	-	-	-	31.68 (0)	A_g R	53.90	70.18